Evidence for glutamate-mediated excitotoxic mechanisms during photoreceptor degeneration in the *rd1* mouse retina

Marie-Noëlle Delyfer,[1,2] Valérie Forster,[1] Nathalie Neveux,[3] Serge Picaud,[1] Thierry Léveillard,[1] José-Alain Sahel[1,4,5]

[1]*Laboratoire de Physiopathologie Cellulaire et Moléculaire de la Rétine, Institut National de la Santé et de la Recherche Médicale (Inserm U592), Université Pierre et Marie Curie, Paris, France;* [2]*Unité des pathologies vitréo-rétiniennes. Service d'Ophtalmologie, Centre Hospitalier Universitaire de Bordeaux, Bordeaux, France;* [3]*Laboratoire de Biochimie A, Hôpital Hôtel-Dieu, AP-HP, Paris, France;* [4]*Centre Hospitalier National d'Ophtalmologie des Quinze-Vingts, Paris, France;* [5]*Institute of Ophthalmology, University College of London, London, United Kingdom*

Purpose: Kinetic studies of photoreceptor cell death in the retinal degeneration (*rd1*) mouse model suggest that photoreceptor degeneration could result from cumulative damage. Since alterations in glutamate metabolism have been described in different models of retinitis pigmentosa, we investigated in the present work whether changes in glutamate turnover occur in the degenerating *rd1* retina and whether glutamate-mediated excitotoxic mechanisms may contribute to rod photoreceptor death in this model.
Methods: Free amino acid levels were quantified in *rd1* and wild-type retinas using an amino acid analyzer selecting times corresponding to early, intermediate, and terminal phases of rod photoreceptor degeneration. Reverse transcription-polymerase chain reaction (RT-PCR) was used to compare the mRNA expression levels of the glial L-glutamate/L-aspartate transporter GLAST, glutamine synthetase (GS), and vimentin, a marker for retinal glia, between *rd1* and wild-type mouse retinas. 6-cyano-7-nitroquinoxaline-2,3-dione (CNQX), an antagonist of both AMPA and kainate subtypes of ionotropic glutamate receptors, was then daily administered from postnatal day 3 (PN3) to PN21 to *rd1* mice while control *rd1* mice received only physiological saline solution (7 per treatment). At PN22, the respective numbers of surviving rods in CNQX- and saline-treated mice were estimated using an unbiased stereological approach.
Results: Gradual increases in free glutamate and glutamine levels were observed during photoreceptor degeneration in *rd1* retinas and were associated with increases in GLAST and GS expression levels. Administration of CNQX induced a statistically significant morphological rescue of rods (>25%, $p<0.05$).
Conclusions: Our data demonstrated that, in the *rd1* mouse retina, photoreceptor degeneration was associated with excessive free glutamate levels and with an upregulation of glutamate turnover (i.e., increases in GLAST, GS, and free glutamine levels). This may indicate that excessive glutamate levels further contribute to rod cell degeneration, thus implying the occurrence of non-cell autonomous mechanisms in the degenerative process in the *rd1* retina.

Retinitis pigmentosa (RP) is a heterogeneous group of inherited retinal degenerative diseases, characterized by the progressive death of rod and cone photoreceptors leading to an irreversible loss of visual function. The retinal degeneration (*rd1*) mouse is an appropriate model for studying the cellular and molecular events leading to photoreceptor death and for evaluating new treatments as the pattern of photoreceptor loss is similar to that in affected humans and because the mutated gene encodes the β-subunit of rod cGMP-phosphodiesterase (Pde6b) [1] as in some affected human families [2]. However, to this day, mechanisms leading to photoreceptor apoptosis still remain unsolved. It has recently been proposed that, in the *rd1* mouse retina, photoreceptor degeneration could result from cumulative damage [3]. It is now well known that the *rd1* mutation results in cGMP accumulation in rods [4].

We can reasonably postulate that such a cGMP accumulation may also induce a continuous depolarization of rod cells by maintaining their cGMP-gated cationic channels open. The subsequent activation of the voltage-sensitive calcium channels could then trigger a prolonged glutamate transmitter release. Changes in amino acid metabolism, and particularly glutamate turnover, have been observed in several different models of inherited retinal degeneration [5-10]. Ulshafer et al. [5] were the first to demonstrate an increase in excitatory amino acid levels (glutamate and aspartate) around degenerating photoreceptors in the *GUCY1** chick. In the RCS rat, Fletcher and Kalloniatis [6-8] observed an increase in aspartate and glutamine levels (both of which are either precursors or metabolites of glutamate), along with alterations in glutamate and GABA manufacturing pathways supposedly linked to abnormal Müller glial cell (MGC) function. In the *rds/rds* mouse, an accumulation of glutamate has also been observed in photoreceptor inner segments [9,10].

Glutamate toxicity has been demonstrated both on inner retinal cells and on photoreceptor terminals [11-18]. In the retina, glutamate homeostasis is maintained by the glial L-glutamate/L-aspartate transporter (GLAST) and by glutamine

Correspondence to: José-Alain Sahel, Laboratoire de Physiopathologie Cellulaire et Moléculaire de la Rétine, INSERM U592-Université Pierre et Marie Curie-Hôpital Saint-Antoine, 184 rue du Faubourg Saint-Antoine, 75571 Paris Cedex 12, France; Phone: (33) 149 284 603; FAX: (33) 149 286 663; email: j-sahel@quinze-vingts.fr

synthetase (GS), both being expressed in MGC [19-24]. Fine tuning of glutamate uptake and degradation in glial cells is essential to avoid neurotoxicity and to allow normal signal transmission between photoreceptor and bipolar cells [19-21].

In the present work, we investigated whether alterations in glutamate metabolism and glutamate-mediated excitotoxic phenomena occur in the degenerating *rd1* retina. The demonstration of such excitotoxic mechanisms could fit with the cumulative damage hypothesis formulated by Clarke et al. [3].

We studied glutamate metabolism in *rd1* and wild-type retinas during the degeneration process by measuring free amino acid levels using an amino acid analyzer. We next analyzed the endogenous response to the observed glutamate increase in *rd1* retina by studying expression levels of GLAST and GS during retinal degeneration. Finally, we investigated whether the observed glutamate increase in the *rd1* retina could contribute to photoreceptor cell death by evaluating the influence of a glutamate receptor antagonist on rod survival.

METHODS

Animals: C3H/He mice (*rd1* mice) and C57BL/6 mice (wild type or controls) were obtained from Iffa Credo (L'Arbresle, France). Animals were cared for and handled according to the Association for Research in Vision and Ophthalmology (ARVO) Statement for the Use of Animals in Ophthalmic and Vision Research. They were maintained in clear plastic cages and subjected to light/dark cycles of 12 h. Day of birth was designated postnatal day 0 (PN0).

Quantification of free amino acids: Retinas were rapidly dissected on ice and deproteinized with 10% (w/v) trichloroacetic acid containing 0.5 mM EDTA. After sonication and centrifugation, supernatants were collected and stored at -80 °C until amino acid analysis. Amino acids were separated and quantified by ion-exchange chromatography using an amino acid analyzer (AminoTac JLC-500/V; JEOL, Tokyo, Japan). The concentrations of each amino acid are expressed, as a percentage, with respect to the sum of all the concentrations of the amino acids quantified by the analyzer (which included taurine, threonine, serine, asparagine, glutamate, glutamine, glycine, alanine, citrulline, valine, isoleucine, leucine, tyrosine, phenylalanine, ornithine, lysine, and arginine).

Reverse transcription-polymerase chain reaction (RT-PCR) analysis: Ten retinas were pooled for each age (PN1, PN8, PN15, PN35) and each strain (*rd1* and control). Total RNAs were purified from retinas by the cesium chloride centrifugation method [25]. cDNAs were synthesized by reverse transcription using random hexamers (pdN$_6$) according to standard protocols. The sequence of each primer, the annealing temperatures, the length of the amplified products, and the GenBank accession numbers are given in Table 1.

Real-time PCRs were performed on a LightCycler instrument (Roche-Diagnostics, Indianapolis, IN) and with SYBR Green I, according to the manufacturer's recommendations. Cycling conditions were as follows: initial denaturation at 95 °C for 2 min, followed by 40 cycles of denaturation at 95 °C for 0 s, annealing for 5 s (see Table 1 for annealing temperatures) and elongation at 72 °C for 15 s. Melting curve analysis

was performed as follows: denaturation at 95 °C for 2 min, annealing at 65 °C for 2 min, followed by a gradual increase (0.1 °C/s) in temperature to 95 °C. Real-time PCR efficiencies were evaluated by calculating the slope of a linear regression graph following recommended protocols. For each experiment, crossing points were calculated by the LightCycler Data Analysis Program (LightCycler-3.5 Software). Target gene expressions were normalized with respect to β-actin expression. Mean crossing point deviations were calculated between samples and controls as specified in the figures.

The amplification steps were performed in triplicate for each point and were repeated using three independent cDNA preparations. The levels of expression of rhodopsin, rod arrestin and of other markers of retinal degeneration were tested and found to be in accordance with the age and genotype analyzed, thus validating our RNA preparations.

Protein extraction and western blotting: rd1 and control mice were killed at PN1, PN8, PN15, PN21, and PN35 (3 animals per age and strain). Eyes were immediately enucleated, and retinas dissected within 2 min in sterile PBS. Retinas were then homogenized in a lysis buffer containing 50 mM Tris-HCl pH 7.5, 1 mM PMSF, 1 mM EDTA, 1 mM dithiothreitol, 1% Triton X-100, 1X mixture of protease inhibitors, 45 µg/ml TLCK, 1 mM sodium fluoride, and 1 mM sodium orthovanadate. Protein concentrations were estimated by Bradford's technique [26]. Proteins were shock-frozen and maintained at -80 °C until analysis. Proteins were further diluted 1:1 in sample buffer (final concentrations: 10 mM Tris-HCl pH 8, 1 mM EDTA, 20 mM dithiothreitol, 3% SDS, 10% glycerol, 0.1% bromophenol blue, 4 M urea) and heated at 50 °C for 45 min. Proteins (10 µg/lane) were separated by 10% SDS-PAGE gel electrophoresis containing 4 M urea, and transferred onto nitrocellulose membranes. Membranes were blocked with PBS, 0.1% Tween 20, 3% nonfat dry milk and 5% horse serum overnight at 4 °C and then incubated with anti-GLAST antibody (1:15000) for 2 h at room temperature. Membranes were then washed and incubated with the appropriate horseradish peroxidase-labeled secondary antibody (1:15000; Jackson ImmunoResearch Laboratories, West Grove, PA) for one hour at room temperature. Antibody binding was visualized by Enhanced Chemiluminescence detec-

TABLE 1. RT-PCR CONDITIONS AND PRIMERS

Gene	Forward and reverse primer sequences	Annealing temperature (°C)	Product length (bp)	GenBank accession number
β-actin	F: AAAGACCTCTATGCCAACACAG R: AAAGAAAGGGTGTAAAACGCAG	57	296	M12481
GLAST	F: GAAGTCTCCCAGACGTTCTAATCC R: GCTCTGAAACCGCCACTTACTATC	58	303	D63816
GLT-1	F: ATGCTCATCCTCCCTCTTATCATC R: CTTTCTTTGTCACTGTCTGAATCTG	56	313	AB007810
GS	F: TGTACCTCCATCCTGTTGCC R: GTCCCCGTAATCTTGACTCC	56	349	U09114
vimentin	F: TTTTGCCCTTGAAGCTGCTAAC R: TCACCTGTCCATCTCTGGTCT	56	314	M26251

This table lists the oligonucleotides used for RT-PCR with the corresponding annealing temperatures, PCR product lengths, and GenBank accession numbers. All these primers were used for real-time PCR.

tion system (ECL+, Amersham, Arlington Heights, IL) as recommended by the manufacturer. To ensure that equal quantities were loaded in each lane, membranes were stripped and subsequently reprobed with monoclonal anti-α-tubulin antibody (1:500; T5168, Sigma, Saint Louis, MO). Band intensities were quantified by scanning densitometry using Phoretix 1D software (Phoretix International, Newcastle-upon-Tyne, UK).

Intraperitoneal injection of 6-cyano-7-nitroquinoxaline-2,3-dione (CNQX): CNQX was dissolved in a 0.9% NaCl solution and injected intraperitoneally at a final concentration of 15 mM. From PN3 to PN21, *rd1* mice received intraperitoneal injections of CNQX (30 mg/kg/day), whereas control *rd1* mice were injected with an equivalent volume of physiological saline solution (vehicle).

Electroretinogram recordings: Electroretinograms (ERGs) were recorded as described previously [27-29]. Postnatal day 22 CNQX- and saline-injected *rd1* mice were dark-adapted for at least 16 h and anesthetized by intramuscular injection of ketamine (100 mg/kg body weight) and xylazine 2% (10 mg/kg body weight). Pupils were dilated with 0.5% tropicamide and the cornea was locally anesthetized with 0.5% oxybuprocaine application. Body temperature was maintained near 37 °C with a heating pad. Upper and lower lids were retracted to proptose and maintain the eye open. Scotopic rod ERGs were recorded in both eyes simultaneously by using a gold loop electrode placed on the corneal surface maintained with 3% methylcellulose gel (one electrode for each eye) and referenced to a stainless steel reference electrode inserted subcutaneously on the head of the animal. A needle electrode inserted in the tail served as ground. A 150 watt xenon lamp in a Ganzfeld stimulator (Multiliner Vision, Jaeger Toennies, Germany) provided the light stimulus (10 cds/m^2). Ten recordings were averaged with an interstimulus interval of 120 s.

Rod immunolabeling and cell counting: CNQX-injected mice and saline-injected mice were sacrificed at PN22. Retinas were removed and fixed in paraformaldehyde (4% in PBS) for 2 h. They were rinsed in PBS, permeabilized in PBS containing 0.1% Triton X-100 for 15 min, saturated in PBS containing 0.1% bovine serum albumin and 0.1% Tween 20 for 20 min and then incubated overnight at 4 °C with a rod photoreceptor-specific monoclonal antibody rho-4D2 (10 μg/ml; gift from D. Hicks). After extensive rinsing, the primary antibody was localized using goat anti-mouse IgG antibody coupled with Alexa Fluor 594 (1:1000; Molecular Probes, Leiden, Netherlands). Retinas were flat-mounted in a 50% PBS-glycerol (1:1) solution with photoreceptors facing up and examined with a Nikon Optophot 2 Epifluorescence microscope. Immunolabeled rods were then quantified using a stereological approach permitting unbiased sampling as previously described [30].

Statistical analysis: All data are presented as the mean and the standard error of the mean (SEM). Unpaired Student's t-test was used to compare amino acid levels in *rd1* mice with controls and to compare rod cell numbers in CNQX-treated *rd1* mice with saline-treated ones. Values of $p<0.05$ were considered to be significant.
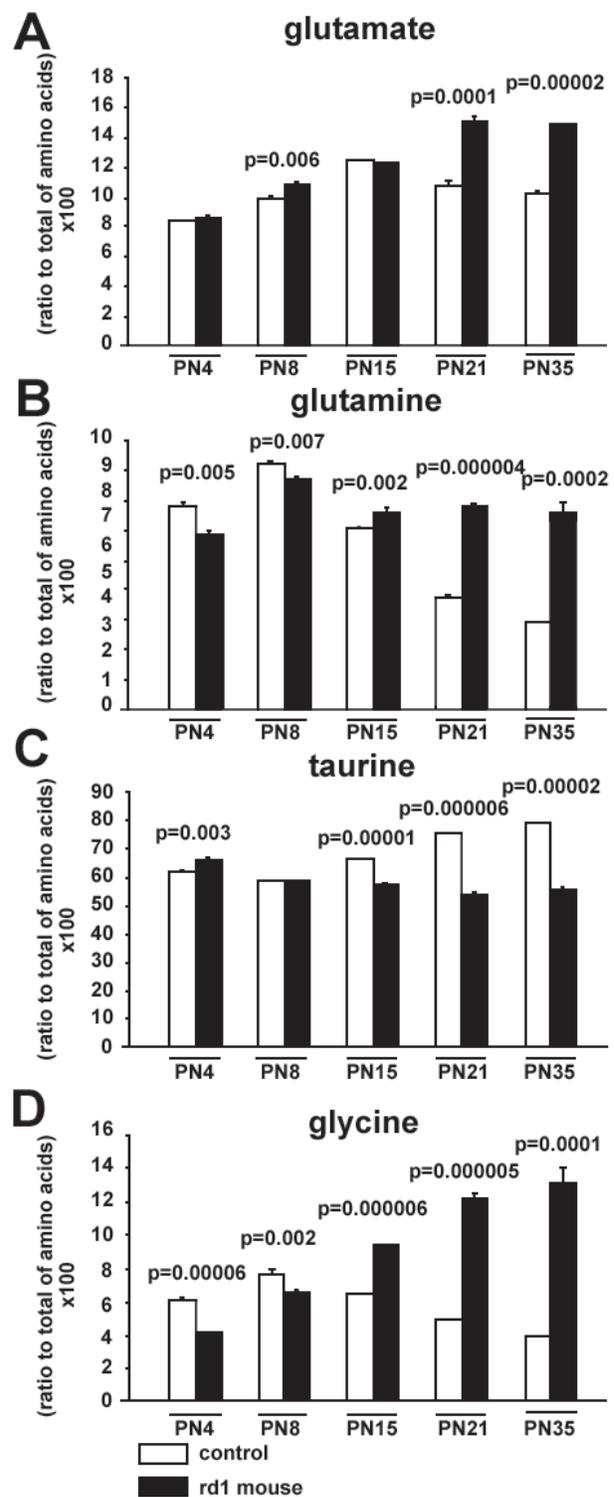

Figure 1. Free glutamate, glutamine, taurine, and glycine levels in *rd1* and control retinas during the degeneration process. Free amino acids were measured in *rd1* and control retinas at PN4, PN8, PN15, PN21, and PN35 using an amino acid analyzer. The concentrations of each amino acid are expressed as a percentage with respect to the sum of all the concentrations of the amino acids quantified by the analyzer. Bars represent the mean (3 for each age and strain); the error bars represent the standard error of the mean. **A**: Glutamate. **B**: Glutamine. **C**: Taurine. **D**: Glycine.

RESULTS

Alterations in amino acid metabolism during photoreceptor degeneration in the rd1 *retina:* As alterations in amino acid levels have already been described in some other models of RP [5-10,31,32], we measured free amino acid levels in *rd1* and control retinas selecting times corresponding to early, intermediate and terminal stages of degeneration. The existing literature indicates that, first, PN8 most likely represents the first time point when the degenerative process becomes detectable in the *rd1* mouse retina [4,33-37], second, PN35 can be considered as the terminal stage of rod degeneration [38], and third, PN15 and PN21 represent intermediate stages between the two. Figure 1 shows that, before the onset of degeneration (from PN4 to PN8), glutamine and glycine levels were lower in *rd1* retinas than in controls, whereas taurine levels were moderately higher in *rd1* retinas than in controls (PN4) and glutamate levels were similar in both strains (PN4). At the onset of degeneration (PN8), glutamate levels were slightly higher in *rd1* retinas, were comparable at PN15 and then steadily increased from PN21 to PN35 with a 1.39 and 1.46 fold difference, respectively (Figure 1A). Glutamine levels were significantly higher in *rd1* retinas than in controls at PN15, PN21 and PN35 with a 1.1-, 1.8 and 2.26 fold difference, respectively (Figure 1B). Taurine levels in control retinas increased progressively from PN8 to PN35, whereas in *rd1* retinas they remained stable from PN8 to PN15 and then slightly decreased (Figure 1C). Glycine levels increased steadily from PN8 to PN35 in *rd1* retinas, whereas they de-
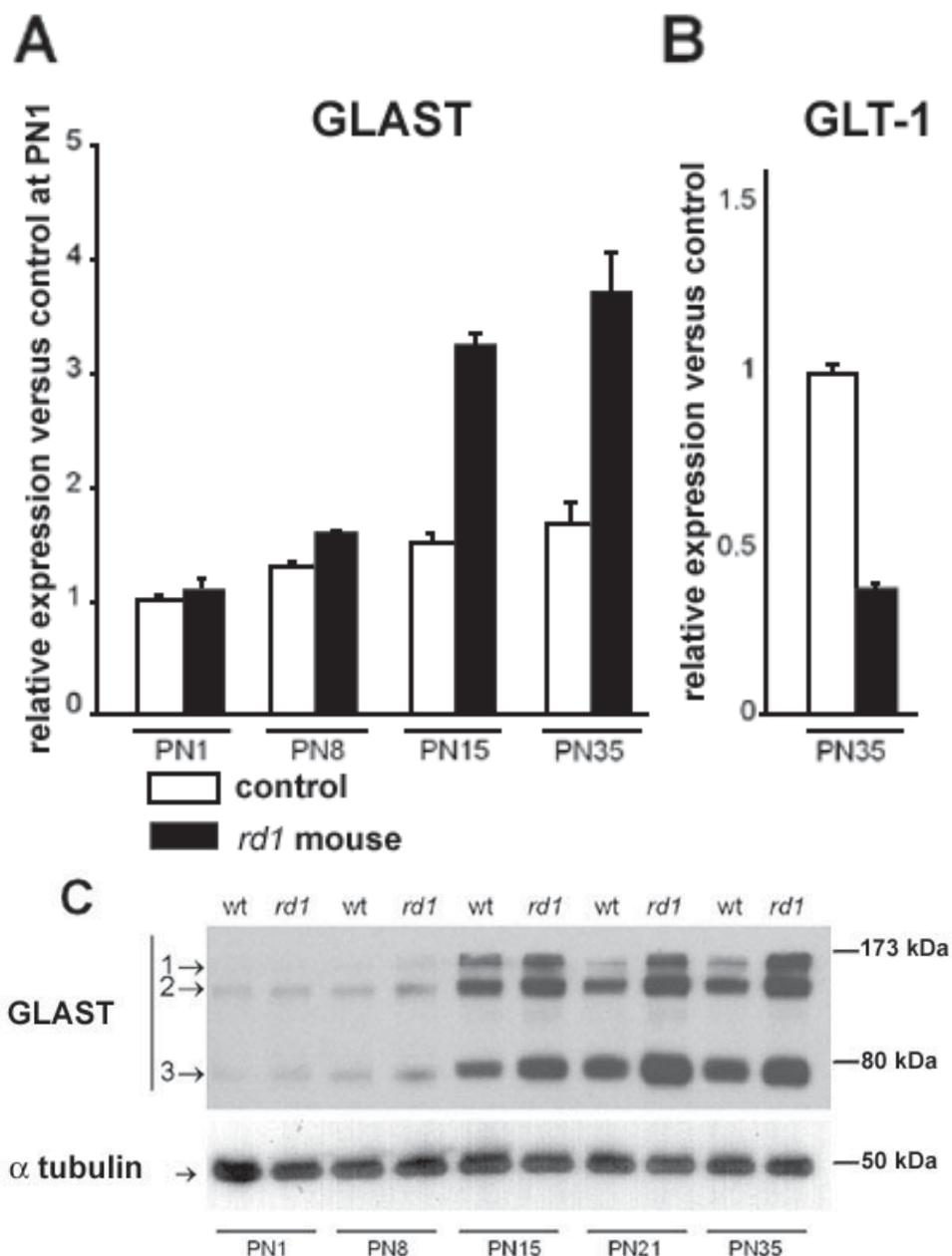

Figure 2. GLAST expression during photoreceptor degeneration. GLAST mRNA expression levels were measured in retinas from untreated *rd1* and control retinas during photoreceptor degeneration. Semi-quantitative analyses of GLAST (**A**) and GLT-1 (**B**) mRNA levels were measured using real-time RT-PCR. Bars represent the mean of triplicate determinations; the error bars represent the standard error of the mean. **C**: Western blots of total protein (10 µg/lane) prepared from *rd1* and control retinas at PN1, PN8, PN15, P21, and PN35, and the blots were probed with anti-GLAST and anti-α-tubulin antibodies. The blots demonstrated bands at about 50 kDa (α-tubulin), at about 76 kDa (GLAST monomeric form, labeled 3), and two bands at about 160 kDa (GLAST multimeric forms, labeled 1 and 2). Results are representative of three independent experiments.

creased in controls (Figure 1D). These results indicate that photoreceptor degeneration is associated with increases in free glutamate, glutamine and glycine and with a decrease in free taurine.

Photoreceptor degeneration induces GLAST upregulation: As glutamate excess has been shown to enhance the expression of GLAST [39-41], a key element in glutamate clearance, we investigated whether the observed increase in free glutamate during rod degeneration in the *rd1* mouse retina (Figure 1A) was associated with a modification in GLAST expression. We measured GLAST mRNA levels in *rd1* and control retinas from PN1 to PN35 by using real-time RT-PCR, selecting times corresponding to early, intermediate and terminal phases of degeneration. Figure 2A shows that at PN1, before the onset of photoreceptor degeneration, no difference in GLAST mRNA expression was observed between *rd1* and control mice. At PN8, GLAST mRNA was 1.24 times higher in *rd1* retinas than in controls. At PN15, GLAST mRNA was 2.15 times more abundant in *rd1* retinas than in controls. It remained at a similar level (2.25 fold difference) at PN35. In contrast, at PN35, photoreceptor degeneration led to a 2.7 fold drop in the glutamate transporter GLT-1 mRNA expression (Figure 2B). This is consistent with GLT-1 being expressed by retinal neuronal cells and more particularly by cones [42]. Western blot analyses (Figure 2C) confirmed that the amount of GLAST protein increased throughout rod degeneration. Though the amount of GLAST protein was the same in the two strains at PN1, at PN8 GLAST was more abundant in the *rd1* mouse and the difference between the two strains increased with time up to PN35. These results demonstrate that GLAST expression increases right from the beginning (PN8) and gradually during the whole rod degeneration process.

Photoreceptor degeneration induces glutamine synthetase upregulation: Given that free glutamate and glutamine levels are increased in *rd1* retinas (Figure 1A,B) and that glutamine synthetase (GS) catalyzes the amidation of glutamate to glutamine, we studied GS mRNA levels in *rd1* and control retinas using real-time RT-PCR. GS mRNA levels were 1.3 fold and 1.52 fold higher in *rd1* mouse retinas than in controls at PN8 and PN15, respectively (Figure 3A). We also measured mRNA levels of vimentin, a marker for retinal glia, in order to check whether the observed increase of GS (and previously of GLAST) did not reflect an increased number of glial cells. No significant differences were observed in vimentin mRNA levels between the two types of retinas at PN8 and PN15 (Figure 3B).

AMPA/kainate-type glutamate receptor antagonist partially rescues presynaptic rod photoreceptor cells: To determine whether the observed free glutamate increase during retinal degeneration (Figure 1A) participates to rod cell death in the *rd1* retina, we studied the effect of a glutamate receptor antagonist (CNQX) on rod cell survival. CNQX or physiological saline solution was daily injected intraperitoneally to *rd1* mice from PN3 to PN21. At PN22, after a 16 h dark adaptation period, scotopic rod ERGs were recorded from saline-treated and CNQX-treated animals just before sacrifice. Retinas were then dissected and immunolabeled with an antibody

that specifically recognized rod photoreceptors. ERG recordings from saline-treated mice were all flat. Although some recordings were detectable from CNQX-treated mice, data from the whole number of animals studied were not statistically significant (data not shown). However, as shown in Figure 4A, a greater number of rods survived in CNQX-treated *rd1* mice in comparison with saline-treated mice. Quantification of surviving rods on whole retinas using a stereological
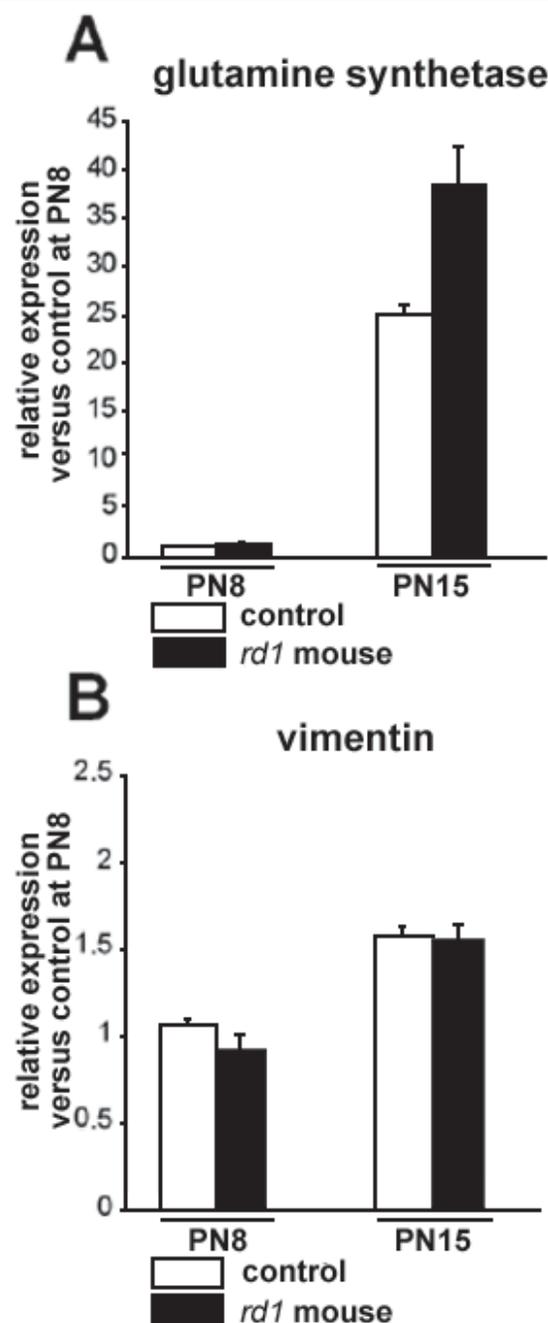

Figure 3. Glutamine synthetase and vimentin mRNA expressions. Glutamine synthetase (**A**) and vimentin (**B**) mRNA levels in *rd1* and control retinas at PN8 and PN15 were measured using real-time RT-PCR. Bars represent the mean of triplicate determinations; the error bars represent the standard error of the mean.

technique demonstrated that there were over 25% more rods in CNQX-treated retinas (2.95 rods per field, SEM 0.50, n=7) than in controls (2.35 rods per field, SEM 0.32, n=7; p<0.05, Figure 4B). Hence, these results indicate that blocking AMPA/kainate ionotropic glutamate receptors can promote morphological survival of rod photoreceptors in the *rd1* mouse.

DISCUSSION

Our results can be summarized as follows: (1) in the *rd1* retina, gradual increases in free glutamate and glutamine levels are observed during photoreceptor degeneration and (2) are associated with increases in GLAST and GS expression levels. (3) Furthermore, administration of a glutamate receptor antagonist induces a statistically significant morphological rescue of rods.

Alterations in glutamate metabolism during photoreceptor degeneration: Alterations in amino acid metabolism have been observed in several different models of inherited retinal degeneration [5-10,31,32,43]. Decreases in taurine content and increases in glycine content have previously been reported in the *rd1* mouse and in the RCS rat retinas [31,32,43]. The decrease in taurine (Figure 1C) can be explained by the loss of photoreceptor cells that have been shown by immunohistochemistry to exhibit high levels of this amino acid [7,31,43]. As for glycine (Figure 1D), its increase has been correlated in the RCS rat to a high increase of glycine immunoreactivity in bipolar cells [7]. Because bipolar cells obtain their glycine from amacrine cells through gap junctions, the glycine increase in bipolar cells has been proposed to be due to a change in gap junction permeability [7]. Concerning glutamate levels, an increase in excitatory amino acid levels around degenerating photoreceptors was observed in the *GUCY1** chick [5], in the RCS rat [6-8] and in the *rds/rds* mouse [9,10]. In the *rd1* mouse, previous work by Orr and colleagues [43] studied glutamate levels during photoreceptor degeneration (along with glycine, taurine and GABA levels) but did not observe any differences in glutamate concentrations between dystrophic and wild-type retinas. Our results indicated an increase in free glutamate in *rd1* retinas with respect to controls (Figure 1A). Since our findings concerning taurine and glycine levels were similar to those reported by Orr et al. [43], the differences in glutamate measurements cannot be explained by the normalization techniques used (their results were expressed on a dry weight basis, whereas in the present study ours were expressed as a proportion of the sum of all the amino acids quantified by the amino acid analyzer, see Methods). The differences in the results are more likely due to the lower resolution of the quantification technique formerly used for glutamate analysis (this technique being different from the ones used for taurine and glycine measurements).

Considering that glutamate toxicity has been demonstrated both on inner retinal cells and on photoreceptor terminals [11-18], we next tried to determine whether the observed glutamate increase could contribute to the rod cell degenerative process.

Evidence for glutamate-mediated toxicity on photoreceptors during retinal degeneration in the rd1 *mouse retina:* In the central nervous system, fast excitatory neurotransmission

is mediated through glutamate acting on ionotropic glutamate receptors [44]. Excessive activation of these receptors leads to neuronal cell death [45]. We therefore studied the effect of an ionotropic glutamate receptor antagonist on rod cell survival in order to know whether the observed glutamate in-
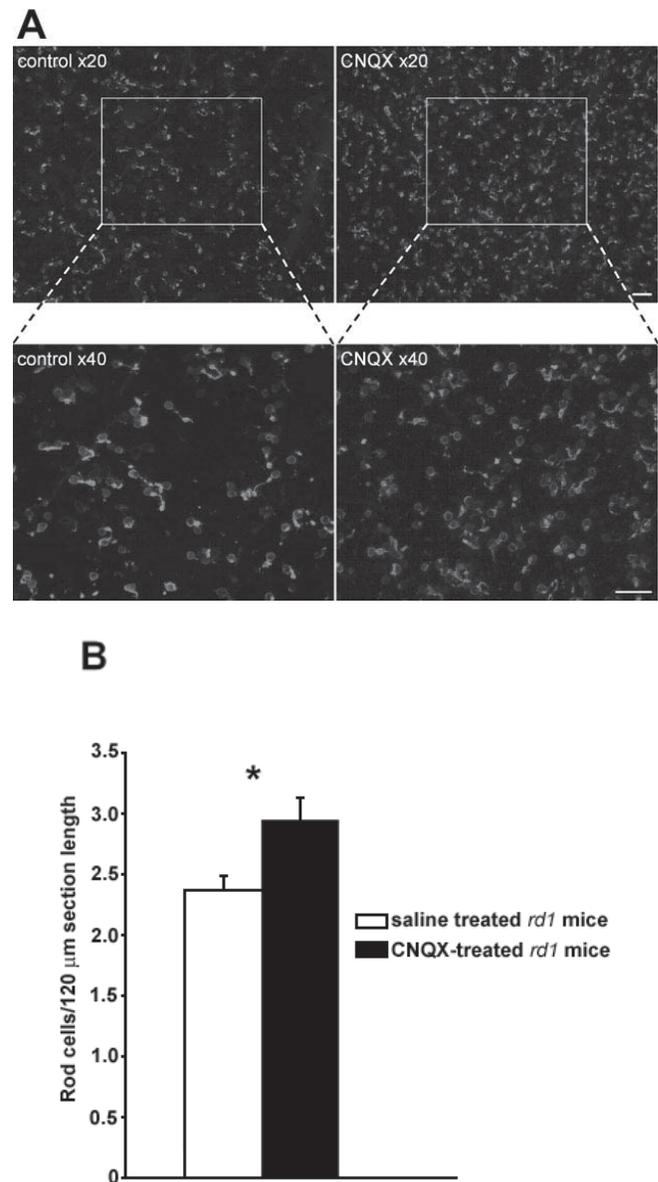

Figure 4. Effect of CNQX on rod survival in the *rd1* retina. CNQX or physiological saline solution was injected daily intraperitoneally to *rd1* mice from PN3 to PN21. After treatment, retinas were dissected, immunolabeled with Rho-4D2, an antibody that specifically recognized rod photoreceptors, and then flat-mounted. **A**: Views of CNQX-treated and saline-treated retinas immunolabeled with Rho-4D2 in an area surrounding the optic nerve head (same distance, same parameters). The greater numbers of surviving rod photoreceptors after CNQX treatment are apparent. The scale bars represent 25 μm. **B**: Results of quantification of immunolabeled rods on whole retinas using a stereological approach. Bars represent the mean (7 animals in each group); the error bars represent the standard error of the mean (an asterisk indicates p<0.05).

crease may contribute to rod death. As shown in Figure 4, CNQX-treated *rd1* mice displayed morphological evidence of rod photoreceptor rescue when compared to saline-treated mice, especially in the area surrounding the optic nerve head. However, such results may seem quite unexpected since ionotropic glutamate receptors are not expressed by photoreceptors [46,47]. In photoreceptors, glutamate has only been reported to elicit a current generated by a transporter coupled to chloride channels [48,49] and to activate some metabotropic receptors, thereby modulating intracellular calcium concentration [50]. These pharmacological data indicate that the CNQX-induced rod rescue cannot be attributed to a direct effect of CNQX on photoreceptors. Considering that expression of ionotropic glutamate receptors in the outer nuclear layer is concentrated at the postsynaptic region, just opposite the presumed site of photoreceptor glutamate release [46,47], our results hence suggested that suppressing glutamate postsynaptic excitation may slow down photoreceptor degeneration. The possibility that glutamate excess may retrogradely affect photoreceptors is further supported by acute and chronic changes detected in photoreceptor outer segments and synaptic terminals following intravitreal injections of kainate in the chicken eye [17].

The glutamate-mediated toxicity hypothesis in the *rd1* mouse concurs with our finding that endogenous neuroprotective mechanisms against glutamate toxicity during rod degeneration were upregulated. Indeed, the two major endogenous mechanisms to protect neurons from glutamate-induced excitotoxicity in the retina and in the CNS are increased glutamate uptake by the glial transporter GLAST [20] along with the subsequent metabolism of glutamate into glutamine by GS selectively expressed in glial cells [23,24]. GLAST expression levels were found to increase throughout photoreceptor degeneration (Figure 2). Comparison of gene expression profiles by microarray analysis in *rd1* and wild-type retinas further confirmed that the gene encoding GLAST is one of the earliest and most highly upregulated genes in the *rd1* retina (data not shown). We also showed that GS mRNA levels increase at PN8 and PN15 in *rd1* retinas (Figure 3A), whereas vimentin mRNAs, also expressed selectively by MGCs in the retina, remain at similar levels in the two strains (Figure 3B). The absence of difference in vimentin mRNA expression between the two strains from PN8 to PN15 strongly indicated that the increase in GS expression, and GLAST, result from neither MGC proliferation nor any concentration phenomenon (due to photoreceptor degeneration) in our *rd1* retina RNA preparations. The GS increase coincided with the increase in free glutamine we observed in the *rd1* mouse retina from PN15 to PN35 (Figure 1B).

However, a persistent glutamate increase while GLAST is upregulated may appear contradictory. Two main hypotheses can be proposed to explain our findings.

First, Rossi et al. [51] reported that during severe ischemia, glutamate release occurs mainly by reversed operation of neuronal glutamate transporters. Although we cannot exclude such a hypothesis, it seems rather unlikely in the present case since

GLAST was not expressed by neurons, and glutamine levels were drastically elevated (Figure 1B). Such a production of glutamine requires efficient capture of glutamate by MGCs through the transporter GLAST, and the subsequent metabolism of glutamate into glutamine via GS activity [24].

We tend to favor the following hypothesis. Glutamate has been demonstrated to proportionally increase GLAST expression in brain-derived astroglial cultures, in primary cultures of cortical astrocytes and recently in retinal MGC cultures [39-41]. We thus propose that the early-observed glutamate increase at PN8 induces GLAST upregulation in the *rd1* retina (Figure 1A and Figure 2). MGCs capture glutamate and convert it into glutamine via GS activity, this neuroprotective mechanism being efficient around PN15 (glutamate levels returned to normal and glutamine levels increased, see Figure 1A,B). Eventually, later during the degenerative process (from PN21 up to PN35), MGC capacity to maintain glutamate homeostasis being overwhelmed, glutamate balance is disrupted (Figure 1A).

Data from Fletcher and Kalloniatis [6] in the RCS rat retina are in line with the latter hypothesis and provide a possible explanation to the eventual incompetence of MGCs in maintaining glutamate balance. By measuring high affinity uptake of ^{3}H-glutamate and the time course of degradation of glutamate within MGC in the RCS retina, Fletcher and Kalloniatis first demonstrated that ^{3}H-glutamate uptake into MGC is greater in the RCS rat retinas than in wild type, in line with the GLAST increase we observed during photoreceptor degeneration in the *rd1* mouse retina (Figure 2). They next showed that glutamate degradation is delayed within MGCs in RCS retinas as compared to wild type. In the RCS rat, as here in the *rd1* mouse, this could be explained by the inhibition of GS activity as an indirect result of glutamine accumulation (Figure 1B) [6,52].

In the CNS, neurotransmitter activity is crucial to regulate synaptic connectivity [53]. The precise role of glutamate in the initial phase of synaptogenesis remains unclear, for example, it could be involved in the stabilization of presynaptic terminals [53]. Perturbation in glutamate levels during a critical period of development may therefore account for abnormal synaptogenesis in the *rd1* mouse. Blanks et al. [37] demonstrated that the first detectable ultrastructural damage in the *rd1* mouse retina is a defective maturation of the outer synaptic layer where abnormal photoreceptor/bipolar cell synaptic contacts are observed. These abnormalities are due to the failure of rod bipolar cells to develop the central element of the post-synaptic triad, implying that the intercellular signaling events necessary for successful contact, synapse formation, and synapse consolidation are impaired in the *rd1* mouse [54]. Thus, we propose that the mutation in the *rd1* mouse resulting in cGMP accumulation in rods [4] may also induce a continuous depolarization of rod cells by maintaining their cGMP-gated cationic channels open. Rod depolarization would then trigger a sustained glutamate transmitter release resulting from the activation of the voltage-sensitive calcium channels. The imbalance of glutamate levels at the synaptic clefts might even-

tually compromise synaptic connectivity and thereby alter subsequent maturation steps of photoreceptors [17,37]. This may lead to "retrograde degeneration" of rods.

Therefore, our data pinpoint the occurrence of additive non-cell autonomous mechanisms contributing to rod photoreceptor death in the *rd1* retina. Glutamate-mediated toxicity may, at least partially, account for the "cumulative damage hypothesis" put forward by Clarke and colleagues [3] in the *rd1* mouse. Blockade of retinal glutamate receptors undoubtedly represents, alone or combined with other therapies, a potential therapeutic approach to prolong photoreceptor survival in RP.

REFERENCES

1. Bowes C, Li T, Danciger M, Baxter LC, Applebury ML, Farber DB. Retinal degeneration in the rd mouse is caused by a defect in the beta subunit of rod cGMP-phosphodiesterase. Nature 1990; 347:677-80.
2. McLaughlin ME, Sandberg MA, Berson EL, Dryja TP. Recessive mutations in the gene encoding the beta-subunit of rod phosphodiesterase in patients with retinitis pigmentosa. Nat Genet 1993; 4:130-4.
3. Clarke G, Collins RA, Leavitt BR, Andrews DF, Hayden MR, Lumsden CJ, McInnes RR. A one-hit model of cell death in inherited neuronal degenerations. Nature 2000; 406:195-9.
4. Farber DB, Flannery JG, Bowes-Rickman C. The rd mouse story: seventy years of research on an animal model of inherited retinal degeneration. Prog Retin Eye Res 1994; 13:31-64.
5. Ulshafer RJ, Sherry DM, Dawson R Jr, Wallace DR. Excitatory amino acid involvement in retinal degeneration. Brain Res 1990; 531:350-4.
6. Fletcher EL, Kalloniatis M. Neurochemical architecture of the normal and degenerating rat retina. J Comp Neurol 1996; 376:343-60.
7. Fletcher EL. Alterations in neurochemistry during retinal degeneration. Microsc Res Tech 2000; 50:89-102.
8. Kalloniatis M, Tomisich G. Amino acid neurochemistry of the vertebrate retina. Prog Retin Eye Res 1999; 18:811-66.
9. Nakazawa M. [A molecular biological study on retinitis pigmentosa]. Nippon Ganka Gakkai Zasshi 1993; 97:1394-405.
10. Noro Y, Ishiguro S, Tamai M. Accumulation of glutamate-like immunoreactivity in the rds/rds mouse retinas. Invest Ophthalmol Vis Sci 1994; 35:1362.
11. Lucas DR, Newhouse JP. The toxic effect of sodium L-glutamate on the inner layers of the retina. AMA Arch Ophthalmol 1957; 58:193-201.
12. Olney JW. Glutamate-induced retinal degeneration in neonatal mice. Electron microscopy of the acutely evolving lesion. J Neuropathol Exp Neurol 1969; 28:455-74.
13. Yazulla S, Kleinschmidt J. The effects of intraocular injection of kainic acid on the synaptic organization of the goldfish retina. Brain Res 1980; 182:287-301.
14. Olney JW. The toxic effects of glutamate and related compounds in the retina and the brain. Retina 1982; 2:341-59.
15. Ingham CA, Morgan IG. Dose-dependent effects of intravitreal kainic acid on specific cell types in chicken retina. Neuroscience 1983; 9:165-81.
16. Sattayasai J, Ehrlich D. Morphology of quisqualate-induced neurotoxicity in the chicken retina. Invest Ophthalmol Vis Sci 1987; 28:106-17.
17. Sattayasai J, Zappia J, Ehrlich D. Differential effects of excitatory amino acids on photoreceptors of the chick retina: an electron-microscopical study using the zinc-iodide-osmium technique. Vis Neurosci 1989; 2:237-45.
18. Sahel JA, Albert DM, Lessell S, Adler H, McGee TL, Konrad-Rastegar J. Mitogenic effects of excitatory amino acids in the adult rat retina. Exp Eye Res 1991; 53:657-64.
19. Derouiche A, Rauen T. Coincidence of L-glutamate/L-aspartate transporter (GLAST) and glutamine synthetase (GS) immunoreactions in retinal glia: evidence for coupling of GLAST and GS in transmitter clearance. J Neurosci Res 1995; 42:131-43.
20. Rauen T, Taylor WR, Kuhlbrodt K, Wiessner M. High-affinity glutamate transporters in the rat retina: a major role of the glial glutamate transporter GLAST-1 in transmitter clearance. Cell Tissue Res 1998; 291:19-31.
21. Harada T, Harada C, Watanabe M, Inoue Y, Sakagawa T, Nakayama N, Sasaki S, Okuyama S, Watase K, Wada K, Tanaka K. Functions of the two glutamate transporters GLAST and GLT-1 in the retina. Proc Natl Acad Sci U S A 1998; 95:4663-6.
22. Izumi Y, Shimamoto K, Benz AM, Hammerman SB, Olney JW, Zorumski CF. Glutamate transporters and retinal excitotoxicity. Glia 2002; 39:58-68.
23. Linser PJ, Sorrentino M, Moscona AA. Cellular compartmentalization of carbonic anhydrase-C and glutamine synthetase in developing and mature mouse neural retina. Brain Res 1984; 315:65-71.
24. Erecinska M, Silver IA. Metabolism and role of glutamate in mammalian brain. Prog Neurobiol 1990; 35:245-96.
25. Glisin V, Crkvenjakov R, Byus C. Ribonucleic acid isolated by cesium chloride centrifugation. Biochemistry 1974; 13:2633-7.
26. Bradford MM. A rapid and sensitive method for the quantitation of microgram quantities of protein utilizing the principle of protein-dye binding. Anal Biochem 1976; 72:248-54.
27. Helmlinger D, Yvert G, Picaud S, Merienne K, Sahel J, Mandel JL, Devys D. Progressive retinal degeneration and dysfunction in R6 Huntington's disease mice. Hum Mol Genet 2002; 11:3351-9.
28. Duboc A, Hanoteau N, Simonutti M, Rudolf G, Nehlig A, Sahel JA, Picaud S. Vigabatrin, the GABA-transaminase inhibitor, damages cone photoreceptors in rats. Ann Neurol 2004; 55:695-705.
29. Mori M, Metzger D, Picaud S, Hindelang C, Simonutti M, Sahel J, Chambon P, Mark M. Retinal dystrophy resulting from ablation of RXR alpha in the mouse retinal pigment epithelium. Am J Pathol 2004; 164:701-10.
30. Frasson M, Picaud S, Leveillard T, Simonutti M, Mohand-Said S, Dreyfus H, Hicks D, Sabel J. Glial cell line-derived neu-

rotrophic factor induces histologic and functional protection of rod photoreceptors in the rd/rd mouse. Invest Ophthalmol Vis Sci 1999; 40:2724-34.

31. Schmidt SY, Berson EL. Taurine uptake in isolated retinas of normal rats and rats with hereditary retinal degeneration. Exp Eye Res 1978; 27:191-8.

32. Okada M, Okuma Y, Osumi Y, Nishihara M, Yokotani K, Ueno H. Neurotransmitter contents in the retina of RCS rat. Graefes Arch Clin Exp Ophthalmol 2000; 238:998-1001.

33. Phelan JK, Bok D. Analysis and quantitation of mRNAs encoding the alpha- and beta-subunits of rod photoreceptor cGMP phosphodiesterase in neonatal retinal degeneration (rd) mouse retinas. Exp Eye Res 2000; 71:119-28.

34. Lasansky A, DeRobertis E. Submicroscopic analysis of the genetic distrophy of visual cells in C3H mice. J Biophys Biochem Cytol 1960; 7:679-84.

35. Shiose Y, Sonohara O [Studies on retinitis pigmentosa. XXVI. Electron micrsocpic aspects of early retinal changes in inherited dystrophic mice]. Nippon Ganka Gakkai Zasshi 1968; 72:1127-41.

36. Caley DW, Johnson C, Liebelt RA. The postnatal development of the retina in the normal and rodless CBA mouse: a light and electron microscopic study. Am J Anat 1972; 133:179-212.

37. Blanks JC, Adinolfi AM, Lolley RN. Photoreceptor degeneration and synaptogenesis in retinal-degenerative (rd) mice. J Comp Neurol 1974; 156:95-106.

38. Carter-Dawson LD, LaVail MM, Sidman RL. Differential effect of the rd mutation on rods and cones in the mouse retina. Invest Ophthalmol Vis Sci 1978; 17:489-98.

39. Duan S, Anderson CM, Stein BA, Swanson RA. Glutamate induces rapid upregulation of astrocyte glutamate transport and cell-surface expression of GLAST. J Neurosci 1999; 19:10193-200.

40. Gegelashvili G, Civenni G, Racagni G, Danbolt NC, Schousboe I, Schousboe A. Glutamate receptor agonists up-regulate glutamate transporter GLAST in astrocytes. Neuroreport 1996; 8:261-5.

41. Taylor S, Srinivasan B, Wordinger RJ, Roque RS. Glutamate stimulates neurotrophin expression in cultured Muller cells. Brain Res Mol Brain Res 2003; 111:189-97.

42. Rauen T, Kanner BI. Localization of the glutamate transporter GLT-1 in rat and macaque monkey retinae. Neurosci Lett 1994; 169:137-40.

43. Orr HT, Cohen AI, Carter JA. The levels of free taurine, glutamate, glycine and gamma-amino butyric acid during the postnatal development of the normal and dystrophic retina of the mouse. Exp Eye Res 1976; 23:377-84.

44. Hollmann M, Heinemann S. Cloned glutamate receptors. Annu Rev Neurosci 1994; 17:31-108.

45. Olney JW, Sharpe LG, Feigin RD. Glutamate-induced brain damage in infant primates. J Neuropathol Exp Neurol 1972; 31:464-88.

46. Morigiwa K, Vardi N. Differential expression of ionotropic glutamate receptor subunits in the outer retina. J Comp Neurol 1999; 405:173-84.

47. Pourcho RG, Qin P, Goebel DJ. Cellular and subcellular distribution of NMDA receptor subunit NR2B in the retina. J Comp Neurol 2001; 433:75-85.

48. Picaud S, Larsson HP, Wellis DP, Lecar H, Werblin F. Cone photoreceptors respond to their own glutamate release in the tiger salamander. Proc Natl Acad Sci U S A 1995; 92:9417-21.

49. Picaud SA, Larsson HP, Grant GB, Lecar H, Werblin FS. Glutamate-gated chloride channel with glutamate-transporter-like properties in cone photoreceptors of the tiger salamander. J Neurophysiol 1995; 74:1760-71.

50. Koulen P, Kuhn R, Wassle H, Brandstatter JH. Modulation of the intracellular calcium concentration in photoreceptor terminals by a presynaptic metabotropic glutamate receptor. Proc Natl Acad Sci U S A 1999; 96:9909-14.

51. Rossi DJ, Oshima T, Attwell D. Glutamate release in severe brain ischaemia is mainly by reversed uptake. Nature 2000; 403:316-21.

52. Feng B, Shiber SK, Max SR. Glutamine regulates glutamine synthetase expression in skeletal muscle cells in culture. J Cell Physiol 1990; 145:376-80.

53. Gan WB. Glutamate-dependent stabilization of presynaptic terminals. Neuron 2003; 38:677-8.

54. Marc RE, Jones BW, Watt CB, Strettoi E. Neural remodeling in retinal degeneration. Prog Retin Eye Res 2003; 22:607-55.